

THE DANISH CENTER FOR APPLIED MATHEMATICS AND MECHANICS

Scientific Council

Leif Christensen	Hydraulic Laboratory
Søren Christiansen	Laboratory of Applied Mathematical Physics
Frank A. Englund	Hydraulic Laboratory
Svend Gravesen	Structural Research Laboratory
Erik Hansen	Laboratory of Applied Mathematical Physics
H. Saustrup Kristensen	Department of Fluid Mechanics
Frithiof I. Niordson	Department of Solid Mechanics
Bent Pedersen	Structural Research Laboratory
P. Terndrup Pedersen	Department of Solid Mechanics
Kristian Refslund	Department of Fluid Mechanics

Secretary

Frithiof I. Niordson, Professor, Ph. D.
Department of Solid Mechanics, Building 404
Technical University of Denmark
2800 Lyngby, Denmark

DESIGNING VIBRATING MEMBRANES

by
John W. Hutchinson
and
Frithiof I. Niordson



DEPARTMENT
OF
SOLID MECHANICS

THE TECHNICAL UNIVERSITY OF DENMARK

DESIGNING VIBRATING MEMBRANES

John W. Hutchinson *)

and

Frithiof I. Niordson

Department of Solid Mechanics

The Technical University of Denmark, Lyngby, Denmark

ABSTRACT - The pure tones of a vibrating membrane depend on the shape of its boundary. A method is presented by which the boundary may be determined from a set of given frequencies. Some cases, which are given as examples, indicate that the gross features of the shape are determined by the first few frequencies. To illustrate the method a "harmonic" drum is designed, which is characterized by the simple rational ratios 2:3:3:4 between the frequencies corresponding to its first four natural modes.

INTRODUCTION

The shape of a vibrating membrane determines the spectrum of its natural frequencies. That is, the shape of a plane region determines the eigenvalues associated with non-trivial solutions to the Helmholtz equation

$$(1) \quad \Delta w + \lambda w = 0,$$

with $w = 0$ on the boundary of the region. The extent to which the frequency spectrum determines the shape is not known. The possibility that the spectrum uniquely determines the shape does not seem implausible, although it has

*) Professor of Applied Mechanics, Harvard University, Cambridge, USA. Visiting at the Technical University of Denmark.

not been proved. Furthermore, there exist examples of one-dimensional eigenvalue problems where analogous uniqueness principles do not hold [1].

Most studies of inverse eigenvalue problems have been motivated by questions that arise in physics and have focused primarily on the asymptotic properties of the eigenvalues. It is known, for example, that the area, length of the boundary, and connectivity of a region can be found from the asymptotic representation of the spectrum of the Helmholtz equation. Results such as these are contained in Ref. [2]-[12]. A very readable account of this work has been given by KAC [12].

In mechanics and especially in engineering applications of mechanics, it is generally true that the low end of the spectrum of eigenvalues is more relevant than the asymptotic range. In the present context, one expects that the gross features of the shape of a vibrating membrane will be tied to the values of the first few natural frequencies. It is this aspect of the inverse eigenvalue problem on which we hope to shed a little light by way of a few examples. Our study is similar in spirit to previous work by Niordson on onedimensional eigenvalue problems [13] and the inverse problem for vibrating plates [14].

In the following section an equation is derived for the rates of change of the eigenvalues of the Helmholtz equation with respect to variations in the shape of the region. This leads to an algorithm for determining shapes for which the first N eigenvalues (counted in proportion to the multiplicity of their eigenfunctions) coincide with N prescribed values. Of course, there is no guarantee that any shape exists for which the first N frequencies take on arbitrarily selected values. For example, we conjecture that for any region the ratio of the second eigenvalue to the first does not exceed the corresponding ratio associated with the circular region, which is approximately 2.5307.

While we have not been able to prove this, we will show that for all near-circular shapes this ratio is less than the value associated with the circle.

The third and fourth sections contain a description of the numerical method, which makes use of a polynomial function of a complex variable to map a given region, assumed to be simply connected, into the unit circle. Eigenvalues are obtained from a modal analysis of the transformed Helmholtz equation. Examples which illustrate how the first few eigenvalues determine detail of shape are presented in the final section. Included there is a shape of a "harmonic" drum which is designed for consonance with its second and third distinct frequencies, having the ratios 3:2 and 4:2, respectively, to the first.

EIGENVALUE VARIATION WITH SHAPE CHANGE AND AN ALGORITHM FOR SOLVING THE INVERSE PROBLEM

Let W be one of the orthonormal eigenfunctions on the region D bounded by the curve C and let λ be the associated eigenvalue. Thus,

$$(2) \quad \Delta W + \lambda W = 0 \quad \text{in } D$$

$$(3) \quad W = 0 \quad \text{on } C$$

and

$$(4) \quad \int_D W^2 dA = 1$$

where $\Delta \equiv \frac{\partial^2}{\partial x^2} + \frac{\partial^2}{\partial y^2}$ denotes the Laplacian operator.

Suppose the boundary C undergoes a slight change such that the new boundary becomes $C + \delta C$ enclosing $D + \delta D$ as shown in Figure 1. We wish to calculate the associated

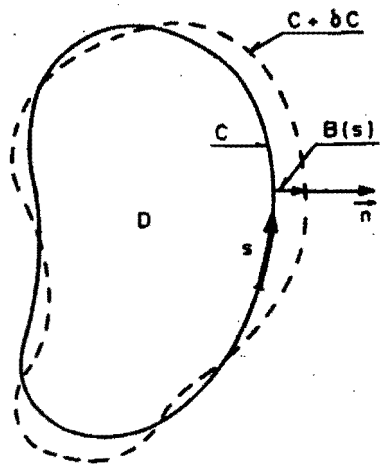


Figure 1.

changes in the eigenvalues and, in particular, in λ as a representative value. To this end we consider the following auxiliary problem.

Let U satisfy

$$(5) \quad \Delta U + \lambda U = 0 \quad \text{in } D$$

with the boundary condition

$$(6) \quad U = -\epsilon b(s) \frac{\partial U}{\partial n} \quad \text{on } C$$

and the normalization condition

$$(7) \quad \int_D U^2 dA = 1$$

Here, ϵ is a small number and $b(s)$ is a given continuous function of the arc length s along the boundary curve C .

Let us assume that if $b(s)$ and C are sufficiently

smooth, Λ and U will depend analytically on ϵ so that we may write

$$(8) \quad \begin{aligned} \Lambda &= \Lambda_0 + \epsilon \Lambda_1 + \dots \\ U &= U_0 + \epsilon U_1 + \dots \end{aligned}$$

for small ϵ . For $\epsilon = 0$, the problem for U coincides with that for W and we take $\Lambda_0 = \lambda$. The eigenfunction U_0 for $\epsilon = 0$ will be some linear combination of the p eigenfunctions associated with λ . If $p = 1$, then $U_0 = W$ without ambiguity. If $p > 1$, the linear combination of eigenfunctions will depend on $b(s)$, but without loss of generality this combination can again be identified as W .

Now,

$$(9) \quad \Lambda = - \int_D U \Delta U dA = \int_D (\nabla U)^2 dA + \epsilon \int_C b(s) \left(\frac{\partial U}{\partial n} \right)^2 ds$$

where the second equality follows from an application of Green's formula and the boundary condition (6). If the expansion for Λ and U are introduced into (9), the first order change in Λ is obtained as

$$(10) \quad \epsilon \Lambda_1 = 2\epsilon \int_D \nabla W \cdot \nabla U_1 dA + \epsilon \int_C b(s) \left(\frac{\partial W}{\partial n} \right)^2 ds$$

Application of Green's formula to the first term on the right hand side of (10), together with (2), yields

$$(11) \quad \int_D \nabla W \cdot \nabla U_1 dA = \int_C U_1 \frac{\partial W}{\partial n} ds + \lambda \int_D W U_1 dA$$

As both U and $W = U_0$ are normalized U_1 has to be orthogonal to U_0 and hence the last term in (11) vanishes. This can be seen directly from the following equality:

$$1 = \int_D U^2 dA = \int_D (U_0 + \epsilon U_1 + \dots)^2 dA = 1 + 2\epsilon \int_D U_0 U_1 dA + \dots$$

On the boundary C , $U_1 = -b \frac{\partial W}{\partial n}$ and thus

$$(12) \quad \epsilon \Lambda_1 = -\epsilon \int_C b(s) \left(\frac{\partial W}{\partial n}\right)^2 ds$$

At this point, the solution to the auxiliary problem for U is applied to the problem for the slight change in the boundary from C to $C + \delta C$. In general, U will not vanish on C since U_0 is zero on C and U satisfies (5). If at a typical point on C , $b(s) < 0$, then U will vanish at a distance ϵb (to first order in ϵ) inward along the normal to C . If $b > 0$, then an analytical continuation of U across C will vanish at a distance ϵb outward along the normal to C . In other words, U is a solution to

$$\Delta U + \lambda U = 0$$

in $D + \delta D$ with $U = 0$ on $C + \delta C$. The boundary C is displayed by $B(s) = \epsilon b(s)$ (to first order in ϵ) along the outward normal to C , as shown in Figure 1. Therefore, if λ_1 is any eigenvalue and W_1 is a corresponding normalized eigenfunction, then a displacement of the boundary $B(s) = \epsilon b(s)$ to $C + \delta C$ will lead to the following first order change in this eigenvalue

$$(13) \quad \delta \lambda_1 = -\int_C B(s) \left(\frac{\partial W_1}{\partial n}\right)^2 ds$$

It does not hurt to emphasize again that if there is a multiplicity of eigenfunctions associated with λ_1 then the combination of these represented by W_1 in (13) must be the limit for $\epsilon = 0$ for a given choice of $b(s)$.

Suppose it is desired to determine a shape change that will bring about prescribed changes $\{\delta \lambda_1\}$ in the set of the first N eigenvalues. It is understood that eigenvalues are counted in proportion to the multiplicity

of the associated eigenfunctions. No restriction is placed on changes in the eigenvalues not in this set. For each eigenfunction W_1 , an influence function f_1 is defined according to

$$(14) \quad f_1(s) = \left(\frac{\partial W_1}{\partial n}\right)^2 \Big|_C$$

If the N influence functions associated with this set are linearly independent then it is easily verified that a shape change that will give the desired increments in the eigenvalues is

$$(15) \quad B(s) = -\sum_{i=1}^N \sum_{j=1}^N C_{ij}^{-1} \delta \lambda_i f_j(s)$$

The symmetric matrix C_{ij} , whose inverse is C_{ij}^{-1} , is given by

$$(16) \quad C_{ij} = \int_C f_i(s) f_j(s) ds$$

It is not possible to prescribe arbitrary increments in the eigenvalues when the influence functions under consideration are linearly dependent. An example of such an exceptional shape is the circle. To see this we need consider only the three eigenfunctions associated with the lowest two eigenvalues of the region enclosed by unit circle, i.e.,

$$W_1 = \frac{\sqrt{2} J_0(\sqrt{\gamma_1} r)}{\sqrt{\pi} J_0'(\sqrt{\gamma_1})}$$

$$\begin{bmatrix} W_2 \\ W_3 \end{bmatrix} = \frac{\sqrt{2} J_1(\sqrt{\gamma_2} r)}{\sqrt{\pi} J_1'(\sqrt{\gamma_2})} \begin{bmatrix} \cos(\theta - \theta_0) \\ \sin(\theta - \theta_0) \end{bmatrix}$$

where the first two eigenvalues for the unit circle are $\gamma_1 = 5.78319$ and $\gamma_2 = 14.68197$. The angle θ_0 will depend on the particular shape change $b(\theta)$. Here, J_n is the Bessel function of the first kind of degree n and the prime denotes differentiation with respect to its argument.

Cylindrical coordinates, r and θ , are employed in the usual manner. The three influence functions are given by

$$f_1 = \frac{Y_1}{\pi}, \quad f_2 = \frac{Y_2}{\pi}(1 + \cos 2(\theta - \theta_0)), \quad f_3 = \frac{Y_2}{\pi}(1 - \cos 2(\theta - \theta_0))$$

These are clearly linearly dependent.

An interesting consequence of this linear dependence is that any small shape change away from the circle will diminish (or at least not increase) the ratio of the second lowest eigenvalue to the lowest. To show this, we note that any shape change can be expressed as

$$B(\theta) = \epsilon b(\theta) = \epsilon \left(\sum_{n=0}^{\infty} b_n \cos n\theta + \sum_{n=1}^{\infty} d_n \sin n\theta \right)$$

Only the Fourier terms b_0 , $b_2 \cos 2\theta$ and $d_2 \sin 2\theta$ will influence the three lowest eigenvalues to first order, and these terms can be combined in the form

$$b_0 + \tilde{b}_2 \cos 2(\theta - \tilde{\theta})$$

where from symmetry considerations $\tilde{\theta}$ may be identified with θ_0 in the expression for W_2 and W_3 . Ratios of the new second and third eigenvalues to the new lowest value are found to be

$$(17) \quad \frac{Y_2 + \delta\lambda_2}{Y_1 + \delta\lambda_1} = \frac{Y_2}{Y_1}(1 - \epsilon \tilde{b}_2) + o(\epsilon^2)$$

and

$$(18) \quad \frac{Y_2 + \delta\lambda_3}{Y_1 + \delta\lambda_1} = \frac{Y_2}{Y_1}(1 + \epsilon \tilde{b}_2) + o(\epsilon^2)$$

Depending on the sign of \tilde{b}_2 , either (17) or (18) yields a lower ratio than Y_2/Y_1 and hence no variation of the circular shape can increase the ratio between the second and the first eigenvalue.

We conjecture that the ratio of the second eigenvalue to the first for any shape is less or equal to the corresponding ratio (2.5387) attained by the circle.

Our conjecture is reinforced by the fact that we were not able to find any counterexample among a fairly wide range of shapes, some of which are given below. We may not be too far out on a limb since quite a few isoperimetric properties are possessed by the circular shape [15].

EIGENVALUE ANALYSIS

Let D be a simply connected region in the complex z -plane ($z = x + iy$). Let $z = \omega(\zeta)$ be a function of the complex variable $\zeta = \xi + i\eta$ that conformally maps D into the region bounded by the unit circle in the ζ -plane. With ξ and η as new independent variables, the Helmholtz equation (1) is transformed to

$$(19) \quad \Delta W + \lambda \rho W = 0$$

where

$$\rho = \left| \frac{dz}{d\zeta} \right|^2$$

with $W = 0$ on $|\zeta| = 1$; and now, $\Delta = \frac{\partial^2}{\partial \xi^2} + \frac{\partial^2}{\partial \eta^2}$.

Thus the problem for finding the natural frequencies and vibration modes of a uniform membrane with a non-circular shape is formally equivalent to a problem for the frequencies and modes of a circular membrane with a non-uniform mass distribution ρ .

In this paper the numerical analysis has been restricted to regions which can be mapped into the unit circle by a polynomial mapping function of the form

$$(20) \quad z = \sum_{n=1}^M a_n \zeta^n$$

where $a_n = \alpha_n + \beta_n$. The origin of the z -plane is contained in D and is mapped onto the origin of the ζ -plane. Pure rotations are suppressed by setting $\beta_1 = 0$. With this representation ρ is given by

$$(21) \quad \rho = \frac{dz}{d\zeta} \frac{d\bar{z}}{d\bar{\zeta}} = \sum_{k=-M+1}^{M-1} P_k(r) e^{ik\theta}$$

where $\zeta = re^{i\theta}$ and $P_k(r)$ is a polynomial in r defined by

$$(22) \quad P_k(r) = \sum_{j=0}^{M+1-k} (k+j+1)(j+1) a_{k+j+1} \bar{a}_{j+1} r^{2j+k}, \quad k \geq 0$$

$$P_k(r) = \bar{P}_{-k}(r), \quad k < 0$$

In the standard notation, $(\bar{\quad})$ denotes the complex conjugate.

Eigenvalues and eigenfunctions associated with a region D are obtained by a Rayleigh-Ritz analysis of the transformed Helmholtz equation (19). Any eigenfunction can be expressed quite generally as

$$(23) \quad W = \sum_{n=-\infty}^{\infty} \sum_{m=1}^{\infty} c_{nm} J_n(\sqrt{\gamma_{nm}} r) e^{in\theta}$$

where $c_{nm} = \bar{c}_{-nm}$.

Now, $\{\gamma_{nm}\}$ is used to denote the set of eigenvalues associated with a uniform circular membrane with unit radius, that is, $\sqrt{\gamma_{nm}}$ is the m th zero of the Bessel function of the first kind of degree n .

A set of coupled algebraic equations for the eigenvalue problem is obtained if (23) is substituted in (19) and if use is made of the orthogonality properties of the Bessel functions. Alternatively, a similar procedure based on the variational principle associated with (19) may be used. The following equations result:

$$(24) \quad \gamma_{ij} [J_i'(\sqrt{\gamma_{ij}})]^2 c_{ij} - 2\lambda \sum_{n=-\infty}^{\infty} \sum_{m=1}^{\infty} \sum_{k=-M+1}^{M-1} c_{nm} F_{nmijk} = 0$$

where

$$(25) \quad F_{nmijk} = \begin{cases} \int_0^1 r J_n(\sqrt{\gamma_{nm}} r) J_i(\sqrt{\gamma_{ij}} r) P_k(r) dr \\ \text{if } i+k+n=0 \text{ or } -i+k+n=0 \\ = 0 \text{ otherwise.} \end{cases}$$

Since $P_k(r)$ is a polynomial in r the integrals (25) can be expressed as sums of integrals of the form

$$(26) \quad \int_0^1 r^p J_n(\sqrt{\gamma_{nm}} r) J_i(\sqrt{\gamma_{ij}} r) dr$$

A real matrix equation of the form

$$(27) \quad (H - \lambda A)c = 0$$

can be obtained by splitting (24) into real and imaginary parts. In (27), H is a diagonal matrix with positive elements, A is a positive definite symmetric matrix and c is a column matrix made up of the ordered real and imaginary parts of the coefficients c_{nm} . A further simple transformation brings (27) to a similar form but with H as the identity matrix. In this form, the power method is ideally suited for numerical evaluation of the N lowest eigenvalues and eigenvectors as long as the eigenvalues are distinct. Otherwise, one of the standard methods can be used to find the eigenvalues and eigenvectors. Equation (27) is truncated in such a way that sufficiently many equations are taken into account to provide the accuracy desired for the first N eigenvalues.

NUMERICAL METHODS FOR SOLVING THE INVERSE PROBLEM

Two procedures were tried out to arrive at shapes whose first N frequencies coincide with N prescribed values. The first was a straightforward implementation of the algorithm described in the second section for expressing a small deflection of the boundary curve, measured by $B(s)$, in terms of the influence functions and desired increments in the eigenvalues. A starting shape is chosen. A sequence of iterations is performed which deforms the initial shape in small increments according to (15) until either a shape with the desired first N frequencies is obtained or it becomes clear that such a shape will not be found, at least not starting from that particular initial shape.

At each iteration step the first N eigenvalues with the associated eigenfunctions and influence functions of the current shape are calculated in the manner described in the previous section. Components of the matrix C_{ij} defined in (16) are obtained by numerical integration. As long as this matrix is non-singular, the set of influence functions are linearly independent. The incremental shape change, $B(s)$, is determined from (15); and finally, increments in the mapping coefficients, δa_n , in (20) are solved for in terms of $B(s)$. Numerical integrations are conveniently carried out on the unit circle in the ζ -plane. Small numerical errors will be present at each step, stemming from, for example, numerical integration or the fact that (15) takes into account only first order terms. Nevertheless, if the method does converge on a shape, the only error involved in the numerical values of the eigenvalues of that shape arises from the truncation of (27). This is also true for the method described next.

The second method bypasses the variational formula (15) and makes use instead of derivatives of the eigenvalues with respect to the mapping coefficients. Shape

changes are obtained by directly incrementing these coefficients. Here again, an initial shape is used to start a sequence of iterations. At each step derivatives of the first N eigenvalues are taken with respect to both the real and imaginary parts of the mapping coefficients, i.e.,

$$\frac{\partial \lambda_i}{\partial \alpha_n}, \quad \frac{\partial \lambda_i}{\partial \beta_m} \quad i = 1, N; \quad n = 1, M; \quad m = 2, M.$$

This is done numerically. Desired increments in the eigenvalues are taken to be proportional to the difference between the prescribed eigenvalues, λ_i^0 , and the eigenvalues associated with the current shape, λ_i . That is,

$$(28) \quad \delta \lambda_i = t(\lambda_i^0 - \lambda_i) \quad i = 1, N$$

where the multiplier t is unity if the current eigenvalues are sufficiently close to the prescribed set but less than unity otherwise to insure that the shape change in each iteration is small.

Selected sets of N unknowns from among the α 's and β 's are used to form linear equations for the increments according to

$$(29) \quad \delta \lambda_i = \sum_n \frac{\partial \lambda_i}{\partial \alpha_n} \delta \alpha_n + \sum_n \frac{\partial \lambda_i}{\partial \beta_n} \delta \beta_n \quad i = 1, N$$

For each set the N increments $\{\delta \alpha_n, \delta \beta_n\}$ are solved for from (29). A supplemental criterion must be applied to choose the set of increments which is actually used to give the next shape in the sequence of iterations that is specified by

$$(30) \quad z = \sum_n [(\alpha_n + \delta \alpha_n) + i(\beta_n + \delta \beta_n)] \zeta^n$$

Of course, sets of increments that yield a nonconformal

mapping function are eliminated from consideration.

One possible criterion is to select the new shape that has the greatest least value of $|dz/d\zeta|$ on its boundary. This criterion works well and has the advantage that it tends to prevent the iteration sequence from leading to a nonconformal mapping representation (as opposed to the first method described, which has no such provision).

Nearly all of the examples presented in the next section were calculated on the basis of the second procedure. Seven complex mapping coefficients were used in the calculations (i.e., $M = 7$), and (27) was truncated to 30 equations in the most accurate calculations by retaining only the 30 real and imaginary parts of the c_{nm} 's associated with the γ_{nm} 's taken in ascending order. We estimate that the lowest frequencies calculated for the examples in the next section are accurate to within 0.1%, while the largest frequencies calculated do not exceed the actual values by more than about 0.5%.

EXAMPLES

For the first example the five lowest eigenvalues of the pear-shaped reference shape, shown as a dashed line curve in Figure 2, were calculated and used as prescribed values. The reference shape has one line of symmetry and is specified by equation (20) with $\alpha_1 = 1$, $\alpha_2 = 0.2$ and $\alpha_3 = 0.2$ and with all other α 's and β 's equal to zero. Eigenvalues for the reference shape are given in the Table.

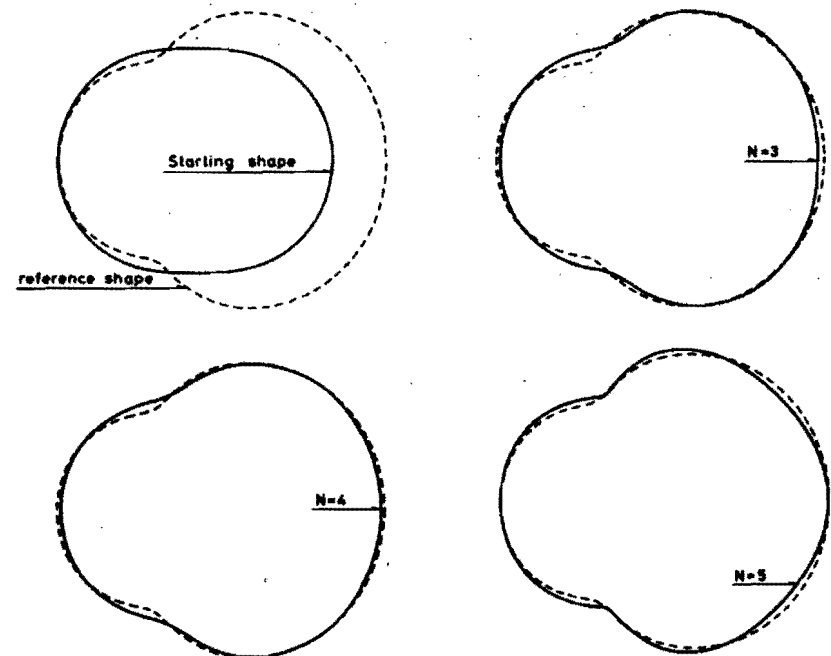


Figure 2.

The shape denoted by $N = 3$ was derived from the starting shape, and its first three eigenvalues are identical to those of the reference. The next shape ($N=4$) has four eigenvalues in common with the reference and the last ($N=5$) has five. In each plot the reference curve is superimposed (with the aid of rigid body translation and rotation) to display the comparison. In this example the search was restricted to shapes with at least one line of symmetry by taking all the imaginary parts of the mapping coefficients to be identically zero. The $N = 3$ shape was used as the starting shape for the $N = 4$ case and similarly the $N = 4$ shape as the first guess for the $N = 5$ case. This procedure proved to be more certain to lead to a shape with, say, five desired frequencies than by starting from an arbitrary initial shape for the $N = 5$ case.

The second example, which is shown in Figure 3, employs Pascal's limaçon (with $\alpha_1 = 1$ and $\alpha_2 = 0.35$) as the reference shape and the results are presented in the same way as in the first example. However, in this case

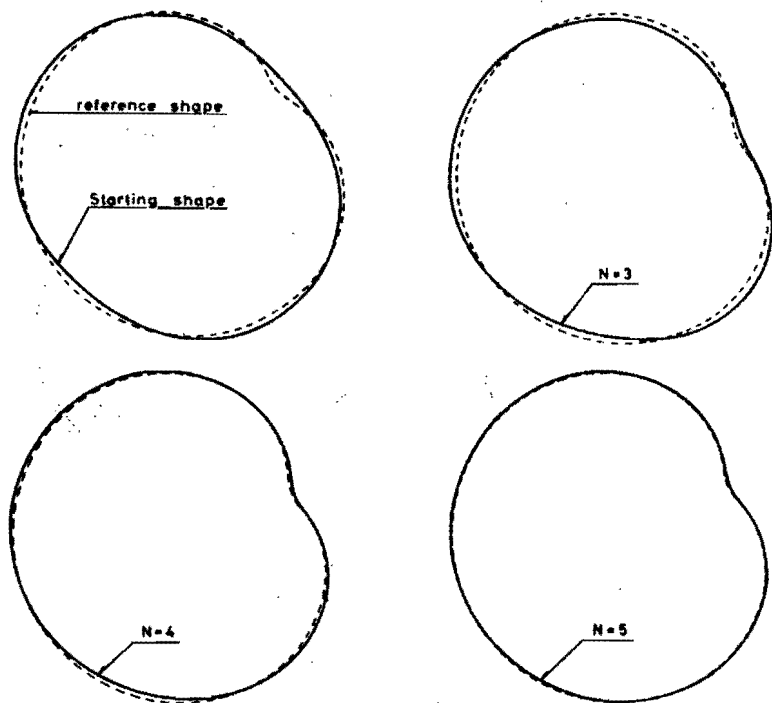


Figure 3.

no symmetry was enforced and the starting shape is asymmetric. Eigenvalues for the reference are also given in the Table.

Our final example is a shape whose second and third distinct frequencies make ratios to the lowest frequency of $3/2$ and 2 , respectively. This shape is shown in Figure 4.

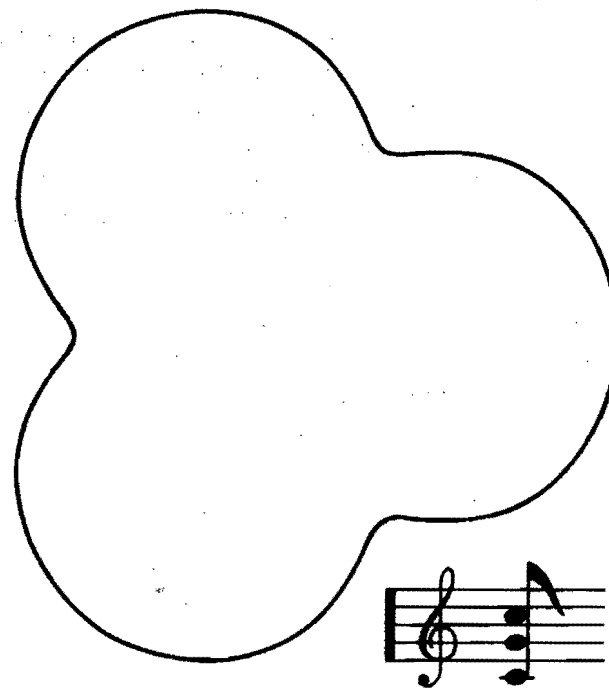


Figure 4.

If a drum with this shape was tuned such that the lowest frequency corresponded to C on the musical scale then the next two notes would be G and C an octave higher. A circular shape has as its corresponding frequency ratios 1.59 and 2.14 , while a square region has 1.58 and 2 .

In searching for this shape we were quite certain that if it did exist it would necessarily have equal second and third eigenvalues (i.e., the second lowest eigenvalue would be associated with two eigenmodes). Thus, we started our search with $N = 4$ and prescribed the eigenvalues such that $\sqrt{\lambda_2/\lambda_1} = \sqrt{\lambda_3/\lambda_1} = 3/2$ and $\sqrt{\lambda_4/\lambda_1} = 2$. By starting from a rather asymmetric initial shape we found a shape very similar to that of Figure 4 with almost perfect 120 degree symmetry. To achieve a more attractive shape with the same

three distinct frequencies, we restricted consideration to shapes with 120 degree symmetry and thereby automatically enforced $\lambda_2 = \lambda_3$ (over the range of shapes considered). This led to the shape of Fig. 4, whose non-zero mapping coefficients are given by $\alpha_1 = 0.9755$, $\alpha_4 = 0.2399$ and $\alpha_7 = 0.0424$ corresponding to a value of $\sqrt{\lambda_1}$ equal to 2.4048.

One might wonder if there exist shapes with 90 degree symmetry with the same first four eigenvalues. A brief search for such a shape convinced us that we would not be able to find one. Indeed, this is consistent with the general impression obtained from the other examples that only four or five eigenvalues suffice to determine the gross features of the shape.

TABLE

SHAPE	$\sqrt{\lambda_1}$	$\sqrt{\lambda_2}$	$\sqrt{\lambda_3}$	$\sqrt{\lambda_4}$	$\sqrt{\lambda_5}$
Unit circle	2.4048	3.8317	3.8317	5.1356	5.1356
Pear-shaped region of Fig.2	2.2388	3.411	3.662	4.539	4.867
Pascal's limaçon of Fig.3	2.1735	3.333	3.575	4.561	4.577
Harmonic drum of Fig.4	2.4048	3.607	3.607	4.809	5.058 (double)

REFERENCES

- [1] FADDEYEV, L.D.: The Inverse Problem in the Quantum Theory of Scattering, J.Math.Phys., Vol. 4 (1963), No. 1.
- [2] WEYL, H.: Das asymptotische Verteilungsgesetz der Eigenwerte linearer partieller Differentialgleichungen, Math. Annalen, Vol. 71 (1912), 441-479.
- [3] WEYL, H.: Ueber die asymptotische Verteilung der Eigenwerte, Kgl. Ges. d. Wiss. Nachrichten. Math.-phys. Klasse (1911), No. 2.
- [4] WEYL, H.: Ueber die Abhängigkeit der Eigenschwingungen einer Membran von deren Begrenzung, J.für Math., Vol. 141 (1912), No. 1, 1-11.
- [5] WEYL, H.: Ueber das Spektrum der Hohlraumstrahlung J.für Math., Vol. 141 (1912), No. 3, 163-181.
- [6] WEYL, H.: Ueber die Randwertaufgabe der Strahlungstheorie und asymptotische Spektralgesetze, J.für Math., Vol. 143 (1913), No. 3, 177-202.
- [7] WEYL, H.: Das asymptotische Verteilungsgesetz der Eigenschwingungen eines beliebig gestalteten elastischen Körpers, Rend.Circ.Matem. Palermo, Vol. 39 (1915), 1-49.
- [8] CARLEMAN, T.: Propriétés asymptotiques des fonctions fondamentales des membranes vibrantes, 8. Skand. Mat. Kongr. (1934), 34-44.
- [9] PLEIJEL, A.: On Green's Functions for Elastic Plates with Clamped, Supported and Free Edges, Proc. Symp. on Spectral Theory and Differential Problems, Stillwater, Oklahoma (1951), 413-454.
- [10] PLEIJEL, A.: A study of certain Green's functions with applications in the theory of vibrating membranes, Arkiv för Mat., 2 (1954) No. 29, 553-569.
- [11] BORG, G.: Uniqueness theorems in the spectral theory of $y'' + (\lambda - q(x))y = 0$, 11. Skand. Mat. Kongr. (1949), 276-287.

- [12] KAC, M.: Can one hear the shape of a drum?, Am. Math. Month. 73, Papers in Analysis, 1-23.
- [13] NIORDSON, F.: A Method for Solving Inverse Eigenvalue Problems, Recent Progress in Appl. Mech., Folke Odqvist Volume, John Wiley & Sons (1967), 373-382.
- [14] NIORDSON, F.: On the Inverse Eigenvalue Problem for Vibrating Plates (in Russian), Problemi Mehaniki tverdovo deformirovannovo tela, Leningrad (1970), 287-294.
- [15] POLYA, G. & SZEGÖ, G.: Isoperimetric inequalities in mathematical physics, Annals of Mathematics Studies, No. 27, Princeton Univ. Press (1951).